

Original Article

Green synthesis of carbon dots from onion juice and ex-situ embedding for antimicrobial/ultraviolet protective nanocellulose films

Negar Nikfarjam¹, Roghayieh Razavi^{2*}, Mehran Moradi², Rahim Molaei³

¹Faculty of Veterinary Medicine, University of Tehran, Tehran, Iran; ²Department of Food Hygiene and Quality Control, Faculty of Veterinary Medicine, Urmia University; ³ Materials Synthesis Laboratory, Carbon Tech Industrial Group, Carbon Tech, Urmia, Iran.

Abstract

Despite the relatively short history of the discovery of carbon dots (C-dots) and the development of their applications, green synthesis methods for nanodots are attracting increasing interest. In this study, green C-dots were synthesized from onion juice using a simple hydrothermal method (200 °C, 4 h), and their optical properties and morphologies were evaluated. The average size of the C-dots was observed to be 7.3 nm. The antibacterial activity of C-dots was assessed against pathogenic bacteria *Escherichia coli* (Gram-negative) and *Listeria monocytogenes* (Gram-positive), with minimum inhibitory concentrations of 8 mg/mL and 4 mg/mL, respectively. Furthermore, the synthesized C-dots were incorporated into nanocellulose using an ex-situ method to produce modified bacterial nanocellulose films with both antimicrobial and ultraviolet (UV) protective properties. The carbon dot-embedded nanocellulose demonstrated enhanced UV-blocking capabilities and greater inhibitory activity against Gram-positive bacteria than Gram-negative bacteria, highlighting its potential as a promising nano-biomaterial for food packaging applications.

Keywords: Antimicrobial, Carbon dots, Nanocellulose, Onion juice.

Introduction

Nanostructures are traditionally categorized into four types based on their critical dimensions: zero-dimensional (0D), one-dimensional (1D), two-dimensional (2D), and three-dimensional (3D) nanomaterials (Wang et al., 2020). Carbon quantum dots, a member of the carbon nanostructure family, belong to 0D nanomaterials because of their small size (less than 10 nm in all dimensions). C-dots exhibit unique physicochemical properties, including chemical inertness, strong photoluminescence,

photostability, antioxidant and antimicrobial activities, low toxicity, and high sustainability (Kousheh et al., 2020). Their surfaces can also be modified with various molecules and functional groups, thereby expanding their applications in bioimaging, sensing, drug delivery, and catalysis (Ghorbani et al., 2021). Recently, C-dots have gained attention in the food industry for enhancing food packaging materials by providing mechanical strength, antioxidant and antimicrobial activities, and UV protection (Kousheh et al., 2020). In addition, they

* **Correspondence:** R. Razavi (razavi.roghayieh13@gmail.com).
<https://doi.org/10.30466/fsp.2025.56060.1006>

Received: 12 March 2025 **Accepted:** 04 May 2025

Available online: 15 May 2025

can serve as nanosensors for monitoring food quality and safety (Khan et al., 2023). C-dots primarily consist of carbon, hydrogen, and oxygen, and their elemental composition is significantly influenced by the synthesis method (Wang et al., 2017). Their properties can be significantly enhanced through heteroatom doping (e.g., nitrogen, sulfur, and phosphorus), enabling tunable photoluminescence with colors ranging from blue to red. The tunable emission depends on the synthetic techniques and the internal structure of the C-dots (Hu et al., 2024).

Biopolymers derived from renewable resources are ecofriendly. BNC serve as ideal hosts for guest molecules, such as antimicrobials, owing to their high water-holding capacity, mechanical strength, and nonparallel nanofiber morphology. Its porous three-dimensional structure enhances its ability to absorb foreign molecules (Rasouli et al., 2021). To date, BNC have been modified using various active ingredients including antibacterial and antioxidant compounds (Kousheh et al., 2020; Salimi et al., 2021).

In recent years, biomass valorization has gained significant attention due to societal awareness and sustainability-focused policies aimed at environmental conservation. Biomass includes the biodegradable portion of products, waste, and residues from biological sources such as agriculture (e.g., plant and animal materials), aquaculture, and related industries (Kurian & Paul, 2021). Most biomass naturally contains heterocycles or heteroatoms, which facilitate effective heteroatom doping of C-dots and enhance their physicochemical properties. C-dots derived from natural sources typically exhibit excellent biocompatibility, biodegradability, availability, hydroxyl-rich structures, and minimal toxicity (Hu et al., 2024).

Previously, our group successfully synthesized a series of biomass-derived C-dots using natural resources such as sour whey (Esmaeili Koutamehr et al., 2023), lemon peel (Semsari et al. 2024), green tea (Khan et al., 2023), turmeric (Roy et al., 2022), and white mulberry (Salimi et al., 2021). These C-dots show promise for food preservation because of their antimicrobial and antifungal properties, antioxidant activity, and light-blocking capabilities. Onion-derived nanoparticles, in particular, offer significant

advantages because of their abundance of ascorbic acid, organosulfur compounds, polyphenols, and essential minerals, such as sulfur, phosphorus, and nitrogen (Monte-Filho et al., 2019).

Dastidar et al. (2021) synthesized and functionalized carbon quantum dots using onion extract and ethylenediamine. The resulting CQDs, which were approximately 1 nm in diameter, exhibited luminescent properties and served as fluorescent probes. The CQDs, decorated with polyhydroxy and amino groups, showed enhanced fluorescence emission (at 325 nm) in the presence of Zn^{2+} ions, whereas other cations (e.g., Fe^{3+} , Pb^{2+} , Cu^{2+} , Ca^{2+} , Hg^{2+}) caused nonspecific fluorescence quenching. Bandi et al. described a hydrothermal method for synthesizing highly fluorescent C-dots using onion waste (Bandi et al., 2016). These C-dots demonstrated high aqueous dispersibility, excitation-dependent fluorescence emission, and stability under varying pH conditions, high ionic strength, and continuous irradiation. The Fe^{3+} ions caused significant fluorescence quenching, enabling the C-dots to function as selective and sensitive nanosensors for detecting Fe^{3+} in real water samples.

In another study, lemon and onion biomasses were used for one-step microwave-assisted carbonization to synthesize highly fluorescent C-dots (Monte-Filho et al., 2019). The results demonstrated efficient fluorescent resonance energy transfer (FRET) between the C-dots (donor) and riboflavin (acceptor). A linear correlation between FRET efficiency and riboflavin concentration has enabled the development of a rapid and accurate analytical method for determining riboflavin levels in multivitamin/mineral supplements. Despite potential interference, the C-dots exhibited selectivity for riboflavin under optimized conditions. Lin et al. produced four types of fluorescent C-dots using red onions, ginger, garlic, and fish as precursors via a hydrothermal approach. The onion-derived C-dots exhibited the most potent antibacterial activity against *Pseudomonas fragi*, with stability across a broad pH range. They also demonstrated antimicrobial properties against both Gram-negative (*Escherichia coli*) and Gram-positive (*Staphylococcus aureus*) bacteria. The minimum inhibitory concentration (MIC) and minimal bactericidal

concentration (MBC) of onion-derived C-dots against *Pseudomonas fragi* were 2 mg/mL and 4 mg/mL, respectively, indicating their potential as bacteriostatic agents for preserving protein-rich foods.

In this study, C-dots were synthesized from white onion (*Allium cepa*) juice using a hydrothermal method and their antimicrobial performance was evaluated. The prepared C-dots were embedded into BNC via an ex-situ procedure, and their antimicrobial properties and UV light-blocking capabilities were assessed. We hypothesized that the onion-derived C-dots would exhibit significant antimicrobial activity against Gram-positive and Gram-negative bacteria because of their surface functional groups (e.g., -OH and -COOH), while the C-dots/BNC Films would demonstrate enhanced UV absorption compared to pure BNC. These properties are expected to synergistically improve the potential of the material for applications in antimicrobial coatings or UV-protective packaging.

Materials and Methods

Chemicals and materials

For the green synthesis of C-dots, white onions were purchased from a local supermarket in Urmia, Iran. All analytical-grade reagents were used without further purification. Freshly distilled deionized water (18.2 M Ω cm) was used throughout the experiments. Microbiological culture media including trypticase soy broth (TSB) and trypticase soy agar (TSA) were obtained from Quelab (Montreal, Canada). *E. coli* (PTCC 1399) and *L. monocytogenes* (PTCC 1298) were sourced from the Iranian Research Organization for Science and Technology (IROST). Additionally, BNC with a purity $\leq 99\%$ contained 98% water, and a thickness of 4 mm was provided by Fanavaran NanoZist Plast Co. (Urmia, Iran). Other reagents and chemicals used in this study were obtained from Sigma-Aldrich company (Saint Louis, MO, USA).

Synthesized of green C-dots

In this study, onion-derived C-dots were prepared by a simple and efficient hydrothermal method. In a typical procedure, 100 mL of pulp-free white onion juice was transferred to a PTFE-lined stainless-steel

chamber and incubated at 200°C for 4 h. After cooling to room temperature, the resulting carbonized product was filtered through filter paper (Whatman No. 42), followed by centrifugation at 18,000 rpm for 20 min. The solution was then centrifuged at 18,000 rpm for 15 minutes. Finally, the purified C-dots were lyophilized and the obtained black powder was stored at 4 °C for further use (Dastidar et al., 2021).

Preparation of C-dots -modified nanocellulose (CD-BNC)

The CD-BNC films were prepared by immersing pre-sterilized (UV light; 2 min) BNC pieces (50 mg) into various concentrations of C-dots (80, 160, 240, and 320 mg/mL) for 24 h at room temperature to obtain loading capacities of 48, 100, 155, and 280 mg/cm³, respectively. After impregnation, the excess free solution on the C-dot-loaded BNC was blotted using filter paper, and the BNC was weighed. The C-dot loading capacity of the BNC was determined spectrophotometrically by measuring the absorbance at 365 nm and calculating the difference in the C-dot concentration before and after impregnation. The results are expressed as the amount of absorbed C-dots per cm³ of dry BNC (Ghorbani et al., 2024).

Instrumental analysis

The UV-Vis absorption of the prepared C-dots and the transmittance of the embedded BNC were measured using a double-beam spectrophotometer (T80+ UV-Vis spectrophotometer PG, Beijing, China) with a resolution of 1 nm over the range of 200–800 nm. The particle size distribution histogram of the synthesized C-dots was analyzed using a Malvern Zetasizer (ZEN 3600 instrument, Malvern Instruments Ltd., UK). The nanodots were morphologically characterized using a transmission electron microscope (TEM) (Leo 906 E, Carl Zeiss, Germany) operated at an accelerating voltage of 120 kV. To investigate the chemical and functional properties of the onion-derived C-dots and confirm their embedding within the BNC framework, Fourier Transform Infrared (FTIR) spectroscopy was conducted using a Thermo Nicolet instrument, Nexus® 670 (USA), in the infrared range of 4000–450 cm⁻¹ with a resolution of 2 cm⁻¹.

Antibacterial activity

Agar diffusion

The antimicrobial properties of the as-prepared C-dots and CD-BNC were evaluated using *E. coli* and *L. monocytogenes* as representative foodborne pathogens. Both bacterial strains were subcultured in TSB from frozen stocks (stored at $-20\text{ }^{\circ}\text{C}$) and incubated at $37 \pm 1\text{ }^{\circ}\text{C}$ for 18 h. The optical density (OD_{600 nm}) of the bacterial suspensions was adjusted to approximately 0.1, corresponding to approximately 8 log CFU/mL . Bacterial counts were confirmed by plating cells on TSA plates and incubating for 24 h at $37 \pm 1\text{ }^{\circ}\text{C}$. The antibacterial activity of C-dots at concentrations of 80, 160, and 240 mg/mL was assessed using the agar well diffusion method, as described by Razavi et al. (2024). An inoculum of $\sim 8\text{ log}_{10}\text{ CFU/mL}$ of bacteria was spread on the plates using a sterilized swab, wells with a diameter of 8 mm were created on agar under sterile conditions, and 100 μL of different C-dot concentrations were added to each well. In addition, the antibacterial properties of the CD-BNC films (100, 155, and 280 mg/cm³) were tested using a disc diffusion antimicrobial assay (Moradi et al. 2021). TSA plates were inoculated with bacterial suspensions and circular modified films (8 mm in diameter) were placed on agar under sterile conditions. The zones of inhibition (ZOI) were measured to evaluate bacterial susceptibility after incubating the plates at $37 \pm 1\text{ }^{\circ}\text{C}$ for 24 h.

MIC and MBC

The MIC and MBC values of the samples were determined using 96-well plates according to the CLSI (2012) guidelines (CLSI, 2012). First, 160 μL of TSB was added to each well, followed by 20 μL of onion-derived C-dots at varying concentrations to achieve final concentrations of 0.5, 1, 2, 4, 8, 16, and 24 mg/mL. Subsequently, 20 μL of bacterial suspension (approximately $1.5 \times 10\text{ CFU/mL}$) was added to each well, and the plates were incubated at $37\text{ }^{\circ}\text{C}$ for 24 h. The MIC and MBC values were determined and verified by microbial plate counting on TSA. The MIC was defined as a 2 log CFU/mL reduction in the initial bacterial inoculum, whereas the MBC was defined as a 3 log₁₀ CFU/mL reduction in the initial bacterial inoculum (Divsalar et al. 2023).

Statistical analysis

Analysis of variance (ANOVA) was used to examine the study's data using GraphPad Prism version 8.4.1 for Windows (San Diego, CA, USA). In addition, Tukey's multiple-range tests were performed to determine whether there were any significant differences ($p < 0.05$) between the groups. All experiments were performed in triplicates.

Results and Discussion

UV-Vis absorption

As shown in the **Figure 1**, the surface plasmon resonance (SPR) bands of the C-dot solution displayed intense light absorption bands (λ_{max}) at 295 nm due to the $\pi\text{-}\pi^*$ transition of C=O or the C=C bonds in the C-dots, which directly correlates with the bright green fluorescence of C-dots. This conjugation enabled effective electron delocalization, making them excellent fluorophores. Additionally, a tail extending (quasi-peak) around 350 nm can be attributed to the C=N and/or C=S bonds ($n\text{-}\pi^*$) present in the structure of the as-synthesized C-dots (Ding et al., 2014). The 350 nm tail confirms the presence of nitrogen/sulfur-containing groups, which enhanced water solubility through polar interactions and provided active sites for antimicrobial activity (as demonstrated in our MIC tests), facilitating conjugation with BNC in subsequent nanocomposite formation. Furthermore, the synthesized C-dot solution appeared bright yellow under white light but emitted bright green fluorescence under UV excitation (**Fig. 1-A**). These observations are consistent with the findings of several previously published studies, which attributed this fluorescence emission to the quantum confinement effect (Ezati et al., 2022; Kousheh et al., 2020).

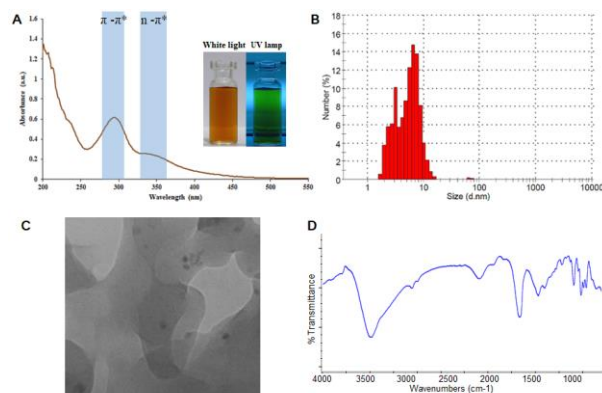


Figure 1. (A) the UV-Vis absorption spectrum, and photographic images of C-dots under white light and the UV lamp, (B) particle size analysis histogram of onion-derived C-dots, (C) TEM micrograph, and (D) FTIR spectrum of as-prepared C-dots.

Size, morphology, and FTIR of onion-derived C-Dots

DLS analysis was performed to determine the average diameter, size distribution, and zeta potential of the synthesized nanodots, dynamic light scattering (DLS) analysis was performed. The obtained results exhibited an average diameter of approximately 7.3 nm and a zeta potential of -14.1 mV, as confirmed by the particle size distribution histogram (**Fig. 1-B**). The negative surface charge values indicate repulsion between the dispersed particles. The larger the surface charge, the stronger is the repulsion, resulting in a more stable colloidal solution (Ahmed et al., 2021). Typically, an absolute value of zeta potential exceeding approximately 30 mV is considered to provide good resistance to particle aggregation owing to the generation of strong electrostatic repulsion (Razavi et al., 2024). Additionally, Figure 1-C shows a representative TEM micrograph of C-dots produced using this green precursor, which reveals that the dots are semi-spherical.

The FTIR spectrum (**Fig. 1-D**), the absorption bands centered at 3426 cm^{-1} correspond to the stretching vibrations of O-H and N-H bonds, while the bands at 3014 , 2933 , and 2842 cm^{-1} are associated with the stretching vibrations of C-H bonds in methyl and methylene groups (Ezati et al. 2022). The bands observed at 2545 cm^{-1} and 2116 cm^{-1} were assigned to the symmetric stretching of S-H and C-N bonds, respectively. Additionally, the strong absorption

peaks at 1633 cm^{-1} and 1484 cm^{-1} can be attributed to the stretching modes of the C=O/C=N and N-H/C-N/COO groups (Hu et al., 2017). The peak at 1219 cm^{-1} was linked to C-N, C-S, and C-O bonds, while the two peaks at 978 cm^{-1} and 891 cm^{-1} were associated with the bending vibrations of C-O-C and C-O bonds. The presence of peaks at 3426 cm^{-1} , indicating the absorption of OH groups and the presence of a strong alcohol group, confirmed the antimicrobial properties of the C-dots (Sukhikh et al. 2022). In addition, the peaks at 1633 cm^{-1} and 1484 cm^{-1} indicate that hydrothermal treatment leads to the formation of sp^2 domains, which, along with the oxygen, hydroxyl, and carboxyl groups present in the sp^3 carbon area, can explain the antibacterial activity of the C-dots (Nguyen et al., 2024).

MIC and MBC

C-dots exhibit antimicrobial properties against bacteria because of their ability to generate reactive oxygen species (ROS), disrupt microbial cell membranes, break down cell structure, cause cytoplasmic leakage, and degrade protein and DNA (Dong et al., 2020). The antibacterial activity of the as-prepared C-dots was assessed against *L. monocytogenes* and *E. coli* using a microdilution method. The MIC and MBC values against *L. monocytogenes* were 4 mg/mL , whereas those against *E. coli* were 8 mg/mL . This could be due to the differences in the cell wall structures of Gram-positive and Gram-negative bacteria. Gram-positive bacteria have a thick peptidoglycan layer but lack an outer membrane, making them more accessible to C-dots. Gram-negative bacteria have an additional outer membrane composed of lipopolysaccharides, which may provide an extra barrier against C-dot penetration (Ezati et al., 2022). In addition, multiple factors influence the antibacterial effectiveness of C-dots. Key determinants include the specific microbial strains involved, the concentration of C-dots, and their intrinsic characteristics such as particle size, surface functional groups, and charge. The peptidoglycan layer in bacterial cell walls contains anionic sites, making it porous and enabling electrostatic interactions with C-dots. Therefore, gram-positive bacteria are generally more susceptible to ROS (Li et al., 2022; Yuan et al., 2021). Divsalar et al. (2023) reported that *L. monocytogenes*

was more sensitive with a MIC/MBC of 0.38 mg/mL, than *Salmonella* Typhimurium with MIC/MBC of 0.76 mg/mL, which is due to the difference in the cell wall structure of microorganisms and interactions between Zn-CDs and cell.

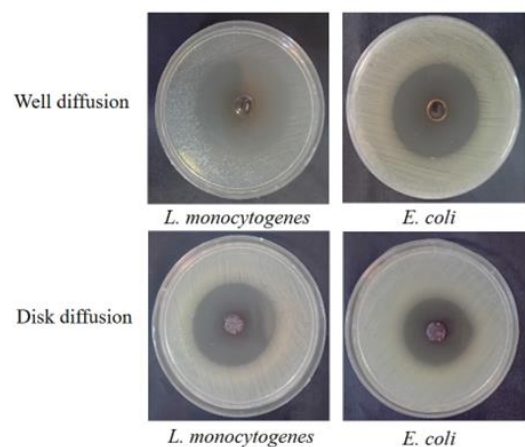


Figure 2. Zone of inhibition of C-dots (240 mg mL^{-1}) and CD-BNC (280 mg cm^{-3}) against *L. monocytogenes* and *E. coli* by well diffusion and disk diffusion methods.

Antimicrobial activity of C-dots and CD-BNCs

The antimicrobial activities of the C-dot and CD-BNC films were further evaluated by measuring the ZOI against *E. coli* and *L. monocytogenes*. **Table 1** and **Figure 2** show the ZOI diameters of the as-prepared C-dots and CD-BNC Films against both microorganisms. The results showed that the selected strains had concentration-dependent antibacterial activity for each of the C-dot and CD-BNC films, such that the most significant antimicrobial activity was observed in *L. monocytogenes* at concentrations of 240 mg/mL , which produced the highest zone of inhibition. In addition, while no antimicrobial activity was observed for pure BNC, modified BNCs loaded with 100 , 155 , and 280 mg/cm^3 of C-dots showed significantly increased inhibitory effects against selected strains of both Gram-positive and Gram-negative bacteria. The ability of C-dots to dissolve in agar media and the immediate hydration of BNC upon contact with the agar surface are likely the key factors driving the release of C-dots into the media. After C-dots bind to bacterial surfaces, they trigger the formation of reactive oxygen species (ROS) through

the transfer of oxygen molecules and creation of free radicals (Jhonsi et al., 2018).

UV-barrier investigation of film

Owing to their unique physicochemical properties, the incorporation of C-dots into a polymer matrix can broaden their potential applications. When C-dots are added to the BNC, they retain their fluorescent properties in the resulting nanocomposite while imparting UV protection to the BNC film matrix. To assess the UV-light barrier properties of BNC films integrated with onion-derived C-dots, BNC films were dried after immersion in C-dot solutions, and the transmittance spectra of the BNC films were recorded in the wavelength range of $200\text{--}800 \text{ nm}$. As shown in **Figure 3**, increasing the number of C-dots in the BNC expanded the light-blocking range, with the transmittance of the BNC film (280 mg/cm^3) decreasing below 1% at wavelengths shorter than 464 nm . **Figure 3** displays photographs of the pure BNC and CD-BNC films under white and UV light. This illustrates the intense green fluorescence of the modified BNCs with as-prepared C-dots. Recent studies have shown that C-dots are highly effective for UV-barrier applications because of their exceptional UV absorption, optical transparency in the visible spectrum, and superior photostability compared with conventional organic absorbers. Their inherent antioxidant properties further enhance UV protection by neutralizing free radicals, whereas their excellent dispersibility allows seamless integration into polymers, coatings, and composites. These attributes make C-dots ideal for advanced sunscreens, UV-blocking packaging, and transparent protective films, combining performance and durability (Arroyave et al., 2021; Khan et al., 2023). In addition, luminescent functionalization of carboxymethyl cellulose films with CDs was reported to convert UV light to blue light (You et al., 2016).

Table 1: Antimicrobial activity (measured by the diameter of inhibition zones in mm) of C-dots and modified BNC films.

| Bacterial strains | C-dots * | | | Modified-BNC** | | |
|-------------------------|--------------------------|--------------------------|--------------------------|--|--------------------------|--------------------------|
| | C-dots (mg/mL) | | | C-dots loading capacity of BNC (mg/cm ³) | | |
| | 80 | 160 | 240 | 100 | 155 | 280 |
| <i>L. monocytogenes</i> | 22.50 ± 1.5 ^c | 27.03 ± 0.5 ^b | 44.12 ± 1.3 ^a | 20.75 ± 1 ^c | 26.86 ± 0.5 ^b | 35.97 ± 1 ^a |
| <i>E. coli</i> | 19.68 ± 0.5 ^c | 24.19 ± 2.5 ^b | 40.91 ± 0.5 ^a | 18.21 ± 0.5 ^c | 22.42 ± 1.5 ^b | 31.11 ± 0.9 ^a |

*According to the well diffusion method. **According to the disc diffusion method. Within each row, values with different letters are significantly different ($p \leq 0.05$).

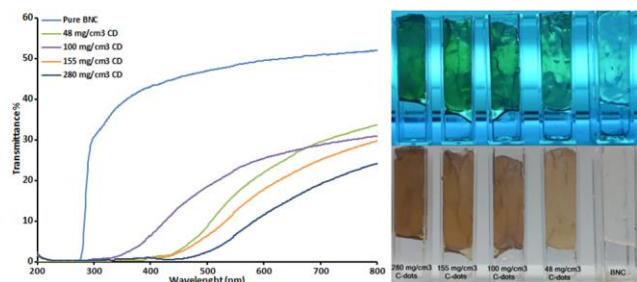


Figure 3. The transmission spectra of BNC and CD-BNC films in the range of 200–800 nm, and the photographs of the BNC and modified BNC membrane with different C-dots loading capacities under white light and UV lamp.

Conclusion

In this study, C-dots were successfully synthesized from white onion juice using a green hydrothermal method, and characterization revealed an average size of 7.3 nm, a zeta potential of -14.1 mV, and functional groups (O-H, N-H, C-H, C=O, and C=N), which contributed to their unique properties. The synthesized C-dots exhibited antimicrobial activity against *L. monocytogenes* (MIC: 4 mg/mL) and *E. coli* (MIC: 8 mg/mL). In addition, embedding C-dots into BNC via an ex-situ procedure enhanced the antimicrobial and UV-blocking properties of the resulting films, with the highest activity at 280 mg/cm³ and transmittance below 1% at wavelengths below 464 nm. This green synthesis approach highlights the potential of onion-derived C-dots and CD-BNC nanocomposites as sustainable, multifunctional materials for food packaging, offering antimicrobial and UV-protective benefits to enhance food safety and shelf life. Future research is needed to optimize and scale these materials for industrial use. To advance this technology for practical implementation, several critical research avenues should be pursued, including validating the antimicrobial efficacy in real food systems under

commercial storage conditions, optimizing production processes for industrial-scale feasibility, conducting comprehensive sensory evaluations for consumer acceptance, and performing thorough toxicological assessments to ensure regulatory compliance and safety. These coordinated efforts will facilitate the transition from laboratory development to commercial application.

Conflicts of Interest

The authors declare that they have no conflicts of interest.

References

- Ahmed, H. B., Abualnaja, K. M., Ghareeb, R. Y., Ibrahim, A. A., Abdelsalam, N. R., & Emam, H. E. (2021). Technical textiles modified with immobilized carbon dots synthesized with infrared assistance. *Journal of Colloid and Interface Science*, *604*, 15–29. <https://doi.org/10.1016/j.jcis.2021.07.014>
- Arroyave, J. M., Ambrusi, R. E., Robein, Y., Pronsato, M. E., Brizuela, G., Di Nezio, M. S., & Centurión, M. E. (2021). Carbon dots structural characterization by solution-state NMR and UV-visible spectroscopy and DFT modeling. *Applied Surface Science*, *564*(2020). <https://doi.org/10.1016/j.apsusc.2021.150195>
- Bandi, R., Gangapuram, B. R., Dadigala, R., Eslavath, R., Singh, S. S., & Guttena, V. (2016). Facile and green synthesis of fluorescent carbon dots from onion waste and their potential applications as sensor and multicolour imaging agents. *RSC Advances*, *6*(34), 28633–28639. <https://doi.org/10.1039/C6RA01669C>
- CLSI. (2012). *Performance standards for antimicrobial disk susceptibility tests; Approved standard—eleventh edition* (11th ed.). CLSI Document M02-A11.
- Ding, H., Wei, J.-S., & Xiong, H.-M. (2014). Nitrogen and sulfur co-doped carbon dots with strong blue luminescence. *Nanoscale*, *6*(22), 13817–13823. <https://doi.org/10.1039/C4NR04267K>
- Divsalar, E., Tajik, H., Moradi, M., & Molaei, R. (2023). Carbon dot-based antimicrobial photosensitizer: Synthesis, characterization and antimicrobial performance against food borne pathogens. *Food Bioscience*, *56*, 103220. <https://doi.org/10.1016/j.fbio.2023.103220>

- Dong, X., Liang, W., Meziani, M. J., Sun, Y.-P., & Yang, L. (2020). Carbon dots as potent antimicrobial agents. *Theranostics*, *10*(2), 671–686. <https://doi.org/10.7150/thno.39863>
- Esmaili Koutamehr, M., Moradi, M., Tajik, H., Molaei, R., Khakbaz Heshmati, M., & Alizadeh, A. (2023). Sour whey-derived carbon dots; synthesis, characterization, antioxidant activity and antimicrobial performance on foodborne pathogens. *LWT*, *184*, 114978. <https://doi.org/10.1016/j.lwt.2023.114978>
- Ezati, P., Rhim, J. W., Molaei, R., Priyadarshi, R., Roy, S., Min, S., Kim, Y. H., Lee, S. G., & Han, S. (2022). Preparation and characterization of B, S, and N-doped glucose carbon dots: Antibacterial, antifungal, and antioxidant activity. *Sustainable Materials and Technologies*, *32*, 397. <https://doi.org/10.1016/j.susmat.2022.e00397>
- Ghorbani, M., Molaei, R., Moradi, M., Tajik, H., Salimi, F., Kousheh, S. A., & Koutamehr, M. E. (2021). Carbon dots-assisted degradation of some common biogenic amines: An in vitro study. *LWT*, *136*, 110320. <https://doi.org/10.1016/j.lwt.2020.110320>
- Ghorbani, M., Moradi, M., Tajik, H., Molaei, R., & Alizadeh, A. (2024). Carbon dots embedded bacterial cellulose membrane as active packaging: Toxicity, in vitro release and application in minced beef packaging. *Food Chemistry*, *433*, 137311. <https://doi.org/10.1016/j.foodchem.2023.137311>
- Ghosh Dastidar, D., Mukherjee, P., Ghosh, D., & Banerjee, D. (2021). Carbon quantum dots prepared from onion extract as fluorescence turn-on probes for selective estimation of Zn²⁺ in blood plasma. *Colloids and Surfaces A: Physicochemical and Engineering Aspects*, *611*, 125781. <https://doi.org/10.1016/j.colsurfa.2020.125781>
- Hu, J., Liao, S., Bai, Y., & Wu, S. (2024). Carbon dots derived from green jujube as chemosensor for tetracycline detection. *Journal of Environmental Chemical Engineering*, *12*(3), 112595. <https://doi.org/10.1016/j.jece.2024.112595>
- Hu, Y., Zhang, L., Li, X., Liu, R., Lin, L., & Zhao, S. (2017). Green preparation of S and N Co-doped carbon dots from water chestnut and onion as well as their use as an Off-On fluorescent probe for the quantification and imaging of coenzyme A. *ACS Sustainable Chemistry & Engineering*, *5*(6), 4992–5000. <https://doi.org/10.1021/acssuschemeng.7b00393>
- Jhonsi, M. A., Ananth, D. A., Nambirajan, G., Sivasudha, T., Yamini, R., Bera, S., & Kathiravan, A. (2018). Antimicrobial activity, cytotoxicity and DNA binding studies of carbon dots. *Spectrochimica Acta Part A: Molecular and Biomolecular Spectroscopy*, *196*, 295–302. <https://doi.org/10.1016/j.saa.2018.02.030>
- Khan, A., Ezati, P., Rhim, J.-W., Kim, J. T., & Molaei, R. (2023). pH-sensitive green tea-derived carbon quantum dots for real-time monitoring of shrimp freshness. *Colloids and Surfaces A: Physicochemical and Engineering Aspects*, *666*, 131242. <https://doi.org/10.1016/j.colsurfa.2023.131242>
- Khan, A., Priyadarshi, R., Bhattacharya, T., & Rhim, J.-W. (2023). Carrageenan/alginate-based functional films incorporated with allium sativum carbon dots for uv-barrier food packaging. *Food and Bioprocess Technology*, *16*(9), 2001–2015. <https://doi.org/10.1007/s11947-023-03048-7>
- Kousheh, S. A., Moradi, M., Tajik, H., & Molaei, R. (2020). Preparation of antimicrobial/ultraviolet protective bacterial nanocellulose film with carbon dots synthesized from lactic acid bacteria. *International Journal of Biological Macromolecules*, *155*, 216–225. <https://doi.org/10.1016/j.ijbiomac.2020.03.230>
- Kurian, M., & Paul, A. (2021). Recent trends in the use of green sources for carbon dot synthesis—A short review. *Carbon Trends*, *3*, 100032. <https://doi.org/10.1016/j.cartre.2021.100032>
- Li, P., Sun, L., Xue, S., Qu, D., An, L., Wang, X., & Sun, Z. (2022). Recent advances of carbon dots as new antimicrobial agents. *SmartMat*, *3*(2), 226–248. <https://doi.org/https://doi.org/10.1002/smm2.1131>
- Monte-Filho, S. S., Andrade, S. I. E., Lima, M. B., & Araujo, M. C. U. (2019). Synthesis of highly fluorescent carbon dots from lemon and onion juices for determination of riboflavin in multivitamin/mineral supplements. *Journal of Pharmaceutical Analysis*, *9*(3), 209–216. <https://doi.org/10.1016/j.jpha.2019.02.003>
- Moradi, M., Kousheh, S. A., Razavi, R., Rasouli, Y., Ghorbani, M., Divsalar, E., Tajik, H., Guimarães, J. T., & Ibrahim, S. A. (2021). Review of microbiological methods for testing protein and carbohydrate-based antimicrobial food packaging. *Trends in Food Science & Technology*, *111*, 595–609. <https://doi.org/10.1016/j.tifs.2021.03.007>
- Nguyen, M. H., Le, A. T., Pham, V. D., Pham, H. M., Do, H. T., Le, D. T., Vu, T. B., & Nguyen, T. B. (2024). A comprehensive study on the antibacterial activities of carbon quantum dots derived from orange juice against Escherichia coli. *Applied Sciences*, *14*(6). <https://doi.org/10.3390/app14062509>
- Rasouli, Y., Moradi, M., Tajik, H., & Molaei, R. (2021). Fabrication of anti-Listeria film based on bacterial cellulose and Lactobacillus sakei-derived bioactive metabolites; application in meat packaging. *Food Bioscience*, *42*, 101218. <https://doi.org/10.1016/j.fbio.2021.101218>
- Razavi, R., Tajik, H., Molaei, R., McClements, D. J., & Moradi, M. (2024). Janus nanoparticles synthesized from hydrophobic carbon dots and carboxymethyl cellulose: Novel antimicrobial additives for fresh food applications. *Food Bioscience*, *62*, 105171. <https://doi.org/10.1016/j.fbio.2024.105171>
- Roy, S., Ezati, P., Rhim, J.-W., & Molaei, R. (2022). Preparation of turmeric-derived sulfur-functionalized carbon dots: antibacterial and antioxidant activity. *Journal of Materials Science*, *57*(4), 2941–2952. <https://doi.org/10.1007/s10853-021-06804-2>
- Salimi, F., Moradi, M., Tajik, H., & Molaei, R. (2021). Optimization and characterization of eco-friendly antimicrobial nanocellulose sheet prepared using carbon dots of white mulberry (L.). *Journal of the Science of Food and Agriculture*, *101*(8), 3439–3447. <https://doi.org/10.1002/jsfa.10974>

Semsari, E., Tajik, H., Molaei, R., & Moradi, M. (2024). Innovative aerosol technology using lemon peel-derived carbon dots for improving shelf life of beef. *Applied Food Research*, 4, 100499. <https://doi.org/10.1016/j.afres.2024.100499>

Sukhikh, S., Prosekov, A., Ivanova, S., Maslennikov, P., Andreeva, A., Budenkova, E., Kashirskikh, E., Tcibulnikova, A., Zemliakova, E., Samusev, I., & Babich, O. (2022). Identification of metabolites with antibacterial activities by analyzing the FTIR spectra of microalgae. *Life*, 12(9). <https://doi.org/10.3390/life12091395>

Wang, D., Wang, Z., Zhan, Q., Pu, Y., Wang, J.-X., Foster, N. R., & Dai, L. (2017). Facile and scalable preparation of fluorescent carbon dots for multifunctional applications. *Engineering*, 3(3), 402–408. <https://doi.org/10.1016/j.ENG.2017.03.014>

Wang, H., Su, W., & Tan, M. (2020). Endogenous fluorescence carbon dots derived from food items. *The Innovation*, 1(1). <https://doi.org/10.1016/j.xinn.2020.04.009>

You, Y., Zhang, H., Liu, Y., & Lei, B. (2016). Transparent sunlight conversion film based on carboxymethyl cellulose and carbon dots. *Carbohydrate Polymers*, 151, 245–250. <https://doi.org/10.1016/j.carbpol.2016.05.063>

Yuan, L., Feng, W., Zhang, Z., Peng, Y., Xiao, Y., & Chen, J. (2021). Effect of potato starch-based antibacterial composite films with thyme oil microemulsion or microcapsule on shelf life of chilled meat. *LWT*, 139, 110462. <https://doi.org/10.1016/j.lwt.2020.110462>